WIND-CSP SHORT-TERM COORDINATION BY MILP APPROACH

*H.M.I. Pousinho *, H. Silva †, V.M.F. Mendes *, †, M. Collares-Pereira *, C. Pereira Cabrita #*

** University of Évora, Évora, and IDMEC/LAETA, Universidade de Lisboa, Lisbon, Portugal;*
email of corresponding author: pousinho@uevora.pt
† Instituto Superior de Engenharia de Lisboa, Lisbon, Portugal
 # University of Beira Interior, Covilha, and CISE, Covilha, Portugal

Keywords: Concentrated solar power; wind power; mixed-integer linear programming; transmission constraints.

Abstract

This paper is on the maximization of total profit in a day-ahead market for a price-taker producer needing a short-term scheduling for wind power plants coordination with concentrated solar power plants, having thermal energy storage systems. The optimization approach proposed for the maximization of profit is a mixed-integer linear programming problem. The approach considers not only transmission grid constraints, but also technical operating constraints on both wind and concentrated solar power plants. Then, an improved short-term scheduling coordination is provided due to the more accurate modelling presented in this paper. Computer simulation results based on data for the Iberian wind and concentrated solar power plants illustrate the coordination benefits and show the effectiveness of the approach.

1 Introduction

Among the renewable energy technology, wind turbine and concentrated solar power (CSP) plant are reported in 2013 as the world's fastest growing energy resources [1]. US and Spain have made notable investment in CSP, with Spain being the leader in CSP deployment. The increased integration of non-dispatchable renewable wind and solar energy into the power grid poses technical challenges on the forecast due to the intermittency and variability of those resources [2].

Typically, wind power plants (WPP) have high variability over the day and low capacity factors [3], meaning that transmission lines sized to transmit the full amount of installed power is mostly unused or underused. Moreover, wind power variability poses problems for system stability, affecting unit commitment decisions, leading to either overcommitment of unneeded reserves, augmenting costs, or undercommitment, decreasing power grid security. So, wind power is to be curtailed [4] and one of the reasons for curtailment is the congestion situations recurrent stressing the lines [5]. Improvements on the use of the existing lines and mitigation on the costs of integrating wind power into power grid, reducing the uncertainty in the power output, requires a coordination between wind power with other energy sources. Several coordination schemes and optimization approaches for short-term scheduling have been investigated, for instances: a wind-thermal coordination scheduling via simulated annealing unveiled an improvement of smoothing the active power fluctuations [6]; a wind-thermal coordination via mixed-integer linear programming (MILP) unveiled a reduction of the uncertainty in wind power output [7]; a coordination of wind power with compressed air energy storage unveiled an improvement due to the synergies between wind power and compressed air energy storage [5]. Also, schemes based on the coordination of wind and hydro power, specially pumped-storage hydro power plants [8,9], unveiled an improvement on minimization of curtailment, energy imbalance and dispatchability. Furthermore, electrical vehicles connection to the power grid are expected to be used as controllable loads and a convenient operation with suitable market design may help accommodate more wind power [10].

Coordination schemes have unveiled progress in reducing of the uncertainty of wind power output by the use of different dispatchable resources or loads, even though resources may not be installed in the same region of WPP deployment. However, to attain this coordination, a novel and accurate wind-CSP scheme is an option followed mainly in regions where the surroundings of the load centres have attractive conditions of wind speed and solar irradiation. The wind-CSP coordination enables to accommodate energy integration into the power grid and electricity markets [11], as well as to increase the dispatchability attribute on that accommodation.

The non-dispatchable characteristic of CPS plants, due to quick changes in output as cloud cover shifts, can be attenuated using thermal energy storage (TES) systems, providing a highly flexible resource of power that can make up for shortfalls in supply from wind power. A CSP plant advantages from having non-expensive TES, allowing dispatchability. TES allows: offsetting generation deficits due to insufficient solar irradiation; shifting power towards suitable periods [12]; reducing real-time net power variability and peak shaving; reducing high marginal cost units due to unpredicted drop in renewable energy [13]; providing ancillary services. Studies on the operation of CSP plant having TES have reported that a CSP producer may earn more profits in the day-ahead market [11,13] and benefits may be expected for the power systems reliability [14].

This paper presents an optimization approach based on MILP to solve the short-term scheduling problem of WPP coordinated with CSP plants, having TES. The goal is to obtain the optimal schedule that maximizes the profit of a price-taker producer taking part in the day-ahead market. The optimization approach, which differs from the above ones, considers not only transmission line constraints, but also technical operating constraints on WPP and on CSP.

The main contributions of this paper can be summarized as follows: 1) The optimal scheduling of WPP with CSP plants having TES; 2) The evaluation of benefits by a comparison between the non-coordination and the coordination scheme considering transmission line constraints; 3) The identification of the added flexibility offered by the TES.

The rest of this paper is organized as follows: Section 2 presents a description of the problem context; Section 3 presents the formulation for the followed approach; Section 4 presents two case studies, comparing schemes of coordination with a non-coordination one; Section 5 concludes the paper.

2 Problem description

2.1 Decision framework

As an overview of the problem, assume a set of wind and CSP plants belonging to a price-taker power producer being able to buy and sell energy in a day-ahead market. The power producer has to take decisions on an hourly basis over a day and needs a schedule to support decisions to maximize profit. Also, assume that the uncertainty about wind and solar power is handled through an artificial neural network (ANN) forecaster [15] and System Advisor Model [16], respectively. While the day-ahead market prices are provided in [17].

2.2 MILP approach

The wind-CSP short-term coordination problem is formulated as a MILP problem given as follows:

$$Max \;\; \boldsymbol{F}(\boldsymbol{x}) = \boldsymbol{f}^{\mathrm{T}}\, \boldsymbol{x} \tag{1}$$

subject to:

$$\underline{\boldsymbol{b}} \le \boldsymbol{A}\,\boldsymbol{x} \le \overline{\boldsymbol{b}} \tag{2}$$

$$\underline{\boldsymbol{x}} \le \boldsymbol{x} \le \overline{\boldsymbol{x}} \tag{3}$$

$$\boldsymbol{x}_j \text{ integer}, \;\; j \in J \tag{4}$$

where $\boldsymbol{F}(\cdot)$ is a linear objective function of the decision variables, $\boldsymbol{f}$ is the vector of coefficients for the linear term, x is the vector of decision variables, $\boldsymbol{A}$ is the constraint matrix, $\underline{\boldsymbol{b}}$ and $\overline{\boldsymbol{b}}$ are the lower and upper bound vectors on constraints, $\underline{\boldsymbol{x}}$ and $\overline{\boldsymbol{x}}$ are the lower and upper bound vectors on variables, $\boldsymbol{x}_j$ are integer variables for $j \in J$.

A MILP approach is an efficient way to determine the optimal wind-CSP coordination scheduling in a reasonable CPU time. The MILP approach is based on a deterministic framework, meaning that future wind and solar power are taken as known data given by the average forecasted values. Hence, the wind-CSP coordination problem may be seen as a sub-problem of a stochastic optimization formulation.

3 Wind-CSP coordination scheduling formulation

The wind-CSP coordination is designed in order to find out in each hour: the thermal power to be charged/discharged for the TES and power selling from the CSP plant to the day-ahead market; the amount of energy storage in TES and storage capacity available; the wind power selling to the day-ahead market. The optimal solution is attained by the maximization an objective function profit subject to constraints as follow.

3.1 Objective function

The objective function provides the profit from the coordination of wind turbines with CSP plants having TES. The profit is equal to the revenues from day-ahead market sales and wind production incentive rate minus the CSP variable costs during the time horizon for the schedule. The objective function to be maximized is given as follows:

$$F = \sum\nolimits_{k \in K} \left[\pi_k^{da} (p_k^s - p_k^b) + \sum\nolimits_{i \in I} \xi\, p_{i,k}^{Wind} - \sum\nolimits_{c \in C} \beta_c\, p_{c,k}^{CSP} \right] \tag{5}$$

In Equation (5), K is the set of hours in the time horizon, π_k^{da} is the forecasted day-ahead market price in hour k, p_k^s is the power sold to day-ahead market in hour k, p_k^b is the power purchased from day-ahead market in hour k, I is the set of wind turbines, ξ is the wind production incentive rate, $p_{i,k}^{Wind}$ is the power output of the wind turbine i, C is the set of CSP plants, β_c is the variable cost of the CSP plant c and $p_{c,k}^{CSP}$ is the power output of the CSP plant c in hour k.

3.2 Constraints

The constraints for the wind-CSP short-term coordination problem are expressed in the form of equality and inequality constraints including simple bounds on the variables.

3.2.1 Transmission grid constraints

The transmission grid constraints are given as follows:

$$(1-\psi)^{-1} p_k^s - (1-\psi) p_k^b = \sum\nolimits_{i \in I} p_{i,k}^{Wind} + \sum\nolimits_{c \in C} p_{c,k}^{CSP} \quad \forall\, k \tag{6}$$

$$-\chi \le (1-\psi)^{-1} p_k^s - (1-\psi) p_k^b \le \chi \quad \forall\, k \tag{7}$$

$$0 \le \sum\nolimits_{i \in I} p_{i,k}^{Wind} + \sum\nolimits_{c \in C} p_{c,k}^{CSP} \le \chi \quad \forall\, k \tag{8}$$

$$0 \le p_k^s \le \chi y_k \quad \forall\, k \tag{9}$$

$$0 \le p_k^b \le \chi (1 - y_k) \quad \forall\, k \tag{10}$$

where ψ is the transmission loss, χ is the transmission capacity, and y_k is a 0/1 variable.

In Equation (6), the electric power balance is enforced between the day-ahead market trading with WPP and CSP plants. In constraints (7) and (8), the electric power bounds are set for the line. In constraints (9) and (10), the energy flow in the line is set infeasible for simultaneously trading by selling and purchasing.

3.2.2 Operational constraints of CSP plants

The operational constraints of CSP plants are given as follows:

$$p_{c,k}^{CSP} = p_{c,k}^{FE} + p_{c,k}^{SE} - X_c \quad \forall\, c,k \tag{11}$$

$$p_{c,k}^{FE} = \eta_1 q_{c,k}^{FE} \quad \forall\, c,k \tag{12}$$

$$p_{c,k}^{SE} = \eta_3 q_{c,k}^{SE} \quad \forall\, c,k \tag{13}$$

$$\underline{Q}_c^{PB} u_{c,k} \le q_{c,k}^{FE} + q_{c,k}^{SE} \le \overline{Q}_c^{PB} u_{c,k} \quad \forall\, c,k \tag{14}$$

$$q_{c,k}^{FE} + q_{c,k}^{FS} \le S_{c,k} \quad \forall\, c,k \tag{15}$$

$$q_{c,k}^{S} = q_{c,k-1}^{S} + \eta_2 q_{c,k}^{FS} - q_{c,k}^{SE} \quad \forall\, c,k \tag{16}$$

$$\underline{Q}_c^{S} \le q_{c,k}^{S} \le \overline{Q}_c^{S} \quad \forall\, c,k \tag{17}$$

$$\underline{Q}_c^{FE} \le q_{c,k}^{FE} \le \overline{Q}_c^{FE} \quad \forall\, c,k \tag{18}$$

$$0 \le p_{c,k}^{CSP} \le \overline{P}_c^{CSP} \quad \forall\, c,k \tag{19}$$

$$p_{c,k}^{SE} - p_{c,k+1}^{SE} \le RD_c^{T} \quad \forall\, c, k = 0,...,K-1 \tag{20}$$

$$\eta_2 (q_{c,k+1}^{FS} - q_{c,k}^{FS}) \le RU_c^{T} \quad \forall\, c, k = 0,...,K-1 \tag{21}$$

$$0 \le p_{c,k}^{SE} \le M\, z_{c,k} \quad \forall\, c,k \tag{22}$$

$$0 \le p_{c,k}^{FS} \le M\,(1 - z_{c,k}) \quad \forall\, c,k \tag{23}$$

$$p_{c,k}^{FE},\ p_{c,k}^{SE},\ q_{c,k}^{FE},\ q_{c,k}^{SE} \ge 0 \quad \forall\, c,k \tag{24}$$

where $p_{c,k}^{FE}$ and $p_{c,k}^{SE}$ are the power produced by the solar field (SF) c and the TES c in hour k, X_c is the parasitic power of the CSP plant c, η_1 is the SF efficiency, $q_{c,k}^{FE}$ is the thermal power from the SF c in hour k, η_3 is the molten-salt tanks efficiency, $q_{c,k}^{SE}$ is the storage power in TES c to produce electricity in hour k, $\underline{Q}_c^{PB}$ and $\overline{Q}_c^{PB}$ are the thermal power bounds of the power block of CSP plant c, $u_{c,k}$ is the CSP plant c commitment in hour k, $q_{c,k}^{FS}$ is the thermal power from the SF c stored in hour k, $S_{c,k}$ is the thermal power produced by the SF c in hour k, $q_{c,k}^{S}$ is the thermal energy stored in TES c at the end of hour k, η_2 is the TES efficiency, $\underline{Q}_c^{S}$ and $\overline{Q}_c^{S}$ are the TES c thermal energy bounds, $\underline{Q}_c^{FE}$ and $\overline{Q}_c^{FE}$ are the thermal power bounds from the SF c, $\overline{P}_c^{CSP}$ is the CSP plant c power bound, RD_c^{T} and RU_c^{T} are the ramp-up and ramp-down limits for charging and discharging the stored energy of TES c, M is a sufficiently large constant $M \ge \overline{P}_c^{CSP}$, and $z_{c,k}$ is the 0/1 variable equal to 1 if TES c discharges power in hour k.

In constraint (11), the electric power balance is enforce between the power output of CSP plant with the electric power produced from the SF, the storage and the parasitic power needed for maintaining the molten-salt fluid in operational conditions. This parasitic power occurs even that a CSP plant is not operating, eventually implying that if producer has not enough energy available, a small quantity of energy is soak up from the grid, incurring on an associated cost. The parasitic power is assumed constant. In constraints (12) and (13), the electric power from the SF and TES is considered dependent on the efficiencies associated with the thermal power of the SF and the storage power, respectively. In constraint (14), the bounds for the sum of the power from the SF and TES are set. In constraints (15) and (16), the balance of the thermal power in the SF and the energy stored in the TES is set, respectively. In constraint (17), the bounds for the thermal power storage in the TES are set in order to avoid the solidification of salts and the maximum storage capacity to be exceeded. In constraint (18), the bounds for the thermal power from the SF are set. In constraint (19), the bounds for the power output of the CSP plants are set. In constraints (20) and (21), the charge and the discharge ramp rates of the TES are set, respectively. In constraints (22) and (23), power restrictions are set to prevent simultaneous discharging and charging of the TES in the same hour, imposed by the 0/1 variable, z_k.

3.2.3 Minimum up/down time constraints of CSP plants

The minimum up/down time constraints of CSP plants are given as follows:

$$\sum_{r=k-UT_c^{SF+T}+1,\ r\ge 1 \in k} (u_{c,r} - u_{c,r-1}) \le u_{c,k} \quad \forall\, c, k = L^{SF+T}+1,\dots,K \tag{25}$$

$$\sum_{r=k-DT_c^{SF+T}+1,\ r\ge 1 \in k} (u_{c,r-1} - u_{c,r}) \le 1 - u_{c,k} \quad \forall\, c, k = F^{SF+T}+1,\dots,K \tag{26}$$

In constraints (25) and (26), the minimum up/down times for the CSP plant c are set based on [18], where $L_c^{SF+T} = \min[K, UT_c^{SF+T}]$ and $F_c^{SF+T} = \min[K, DT_c^{SF+T}]$.

3.2.4 Operational constraints of WPP

The operational constraints of WPP are given as follows:

$$0 \le p_{i,k}^{Wind} \le W_{i,k} \quad \forall\, i,k \tag{27}$$

$$0 \le p_{i,k}^{Wind} \le \overline{P}_i^{Wind} \quad \forall\, i,k \tag{28}$$

where $W_{i,k}$ is the scheduled of wind turbine i in hour k, and $\overline{P}_i^{Wind}$ is the wind turbine i power bound.

In constraint (27), the operating limits for the scheduled wind power of each wind turbine i are set. In constraint (28), the maximum power capacity of each wind turbine i is set.

The developed application for the wind-CSP coordination scheme allows a coding in any computing language interfacing with an optimization solver able to solve MILP problems, for instance, GAMS/CPLEX 12.1. The main

procedures for the wind-CSP are presented in the flowchart shown in Fig. 1.

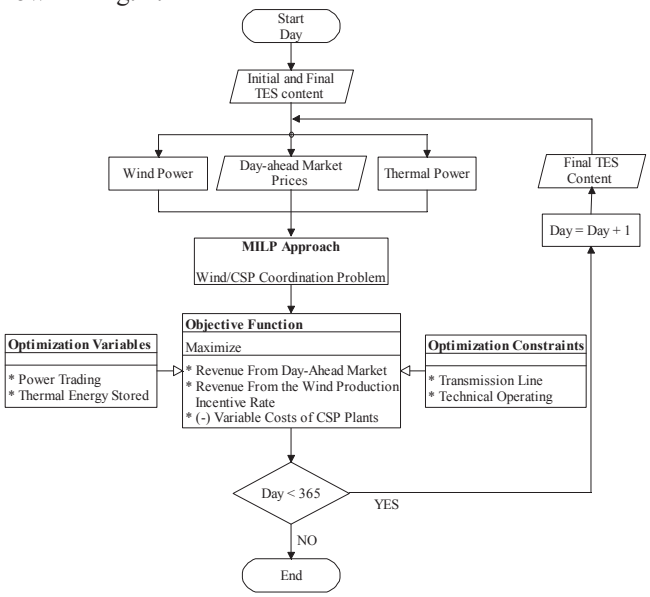

Figure 1: Flowchart of the wind-CSP coordination scheme.

4 Simulation results

The optimization approach modelled as a mixed-integer linear program has been solved using CPLEX 12.1 solver under GAMS environment [19]. The simulations were carried out on a computer with 8 GB RAM with 2.30 GHz CPU.

Realistic case studies based on Iberian wind-CSP system with 40 wind turbines, $i = 1,\ldots,40$, and 2 CSP plants, $c = 1, 2$ having been carried out. The technical data for plants to illustrate the simulation results are shown in Table 1.

Parameters	Values
$\underline{P}_i^{Wind}$ / $\overline{P}_i^{Wind}$ (MW)	0 / 2
$\underline{P}_c^{CSP}$ / $\overline{P}_c^{CSP}$ (MW_e)	0 / 50
$\underline{Q}_c^{S}$ / $\overline{Q}_c^{S}$ (MWh_t)	45 / 700
$\underline{Q}_c^{FE}$ / $\overline{Q}_c^{FE}$ (MW_t)	0 / 150
$\underline{Q}_c^{PB}$ / $\overline{Q}_c^{PB}$ (MW_t)	50 / 125
$q_{c,0}^{S}$ (MWh_t)	120
RU_c^{T} / RD_c^{T} (MW_e/h)	35 / 80
UT_c^{SF+T} / DT_c^{SF+T} (h)	2 / 2

Table 1: Wind-CSP system data.

All WPP have the same data as well as CSP plants. The installed wind power capacity is 80 MW and for CSP is 100 MW_e. The plants share a line connecting to the power grid, having 3 % of losses and the exported power is between 50 MW and 130 MW. The CSP plant module efficiencies are: 1) $\eta_1 = 0.40$; 2) $\eta_2 = 0.35$; 3) $\eta_3 = 0.80$. The parasitic power is 3.5 MW_e. The wind production incentive rate is 35 €/MWh.

The time horizon chosen in the simulations is a day on an hourly basis, corresponding to a participation in a day-ahead market. Within the time horizon are considered as input data not only the solar and the wind power profiles, but also the day-ahead market prices profile. The solar irradiation profile derived from the System Advisor Model [16] was converted into an available thermal power. The wind power profile is derived from the ANN forecaster designed in [15]. The wind power and thermal power output profiles respectively are assumed to be the same for each wind turbine and CSP plant as is shown in Fig. 2.

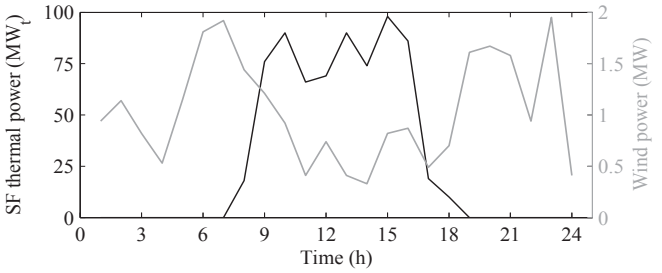

Figure 2: SF thermal and wind power profiles.

Several forecasters are used for forecasting market prices, but for the short-term self-scheduling problem of the wind-CSP coordination the market prices are considered as deterministic input data. So, the Iberian electricity market energy prices in [17] are used and shown in Fig. 3.

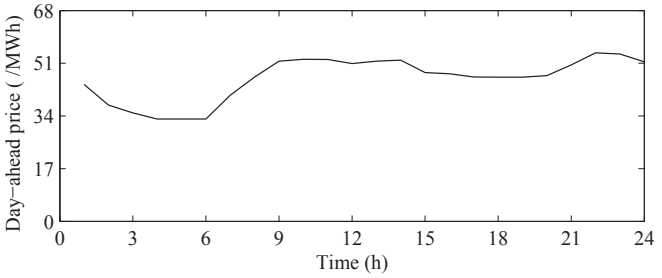

Figure 3: Day-ahead energy market prices.

The effectiveness of the optimization approach applied for solving the optimal self-scheduling is illustrated using simulations on two case studies, namely: Case 1) scheduling for CSP plants with TES; Case 2) scheduling for wind-CSP coordination with TES.

A summary of the case studies showing the number of constraints, continuous variables, binary variables and computation times is shown in Table 2.

#	Case 1	Case 2
Constraints	476	1,436
Continuous variables	384	864
Binary variables	120	120
CPU time (s)	2	8

Table 2: Optimizing characteristics of each case.

3.1 Results obtained for Case 1

This case only considers two CSP plants with TES with a total capacity of 100 MW_e. The energy and profit for the transmission capacity of $\chi = 60$ MW are shown in Table 3.

#	Energy stored (MWh)	Energy sold (MWh)	Profit (€)
Case 1	7,229	566.27	16,888

Table 3: Energy and profit for $\chi = 60$ MW.

The optimal schedule for the set of the CSP plants having TES is shown in Fig. 4.

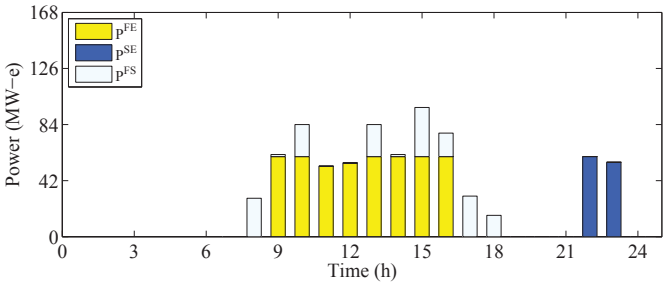

Figure 4: Self-scheduling for CSP plants with TES considering $\chi = 60$ MW.

Fig. 4 shows that CSP having TES introduce dispatchability, allowing the thermal energy collected to be shifted and to fill-in the transmission line in order to increment the capacity factor during lower-source hours with a convenient price. Approximately 30 % of the thermal energy collected by the SF is stored in hours 8, 9 and 10 and in hours 14 to 18 to be into production in hours 22 and 23 when market prices rise. This behaviour allowed by the availability of the TES allows an added improvement on the profit.

3.2 Results obtained for Case 2

This case exploits the synergies between WPP and CSP plants having TES and proves the proficiency of the proposed approach. The number of installed wind turbines and CSP plants having TES are 20 and 2, respectively. The total installed capacities of WPP and CSP plants having TES are 80 MW and 100 MW_e, respectively. The energy and profit for the transmission capacity of $\chi = 60$ MW and $\chi = 130$ MW associated with the enforced system are shown in Table 4.

#	Transmission capacity (MW)	Energy stored (MWh)	Energy sold (MWh)	Profit (€)
Case 2	60	6,405	1,259	83,527
	130	6,269	1,544	95,673

Table 4: Energy and profit for different transmission capacities.

Table 4 allows a comparison between the profits, revealing a reduction of about 15% for $\chi = 60$ MW. Table 4 shows that an increase in the transmission capacity of the line allows to make a better use of the energy stored, allowing an augmented profit.

The optimal schedule for the wind-CSP coordination in what regards the assessing of the impact of transmission constraints with $\chi = 60$ MW and with $\chi = 130$ MW are respectively shown in Fig. 5 (a) and (b).

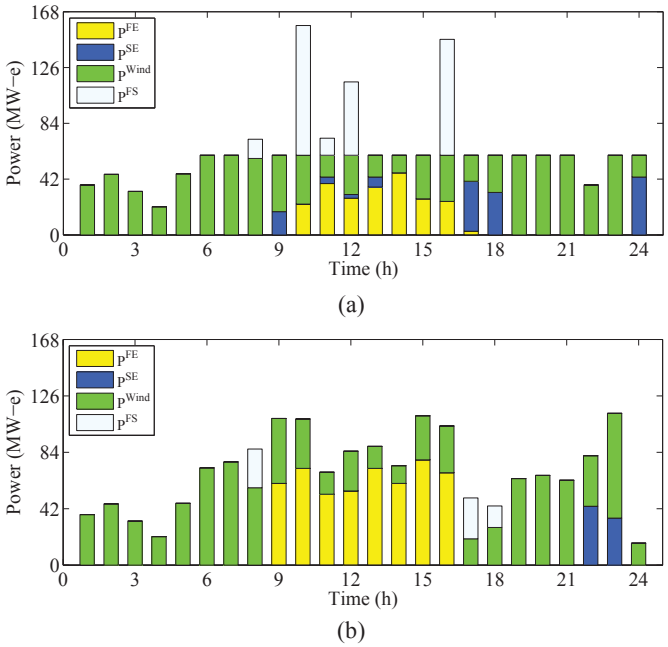

Figure 5: Self-scheduling for wind-CSP coordination, having TES, with different transmission capacities: (a) $\chi = 60$ MW; (b) $\chi = 130$ MW.

Fig. 5 (a) shows for the high price hours a significant CSP production in comparison with low price hours. The benefit of TES shifting the production is revealed, where the excess energy eventually overloading transmission from hours 8, 10 to 12 and 16 is able to be stored for a convenient discharge at hours 11 to 13, 17, 18 and 24. Additionally, the features between wind and solar energies allows for the possibility of enhancement for the scheduling due to the negative correlation. Thus, an efficient energy schedule is obtained, illustrating the proficiency of the optimization approach for accommodating this deployment with different changing patterns of renewable energy in a power system grid.

The thermal energy storage shows the significance of the line capacity regarding the storage in the TES, for instance, the increase in the line capacity raises the level of the storage in the low prices hours with solar thermal power in order to be conveniently used during the other hours. The capacity factor is incremented by downsizing the transmission, causing curtailment and consequent decrease of the energy produced. The thermal energy storage for different transmission capacities are shown in Fig. 6.

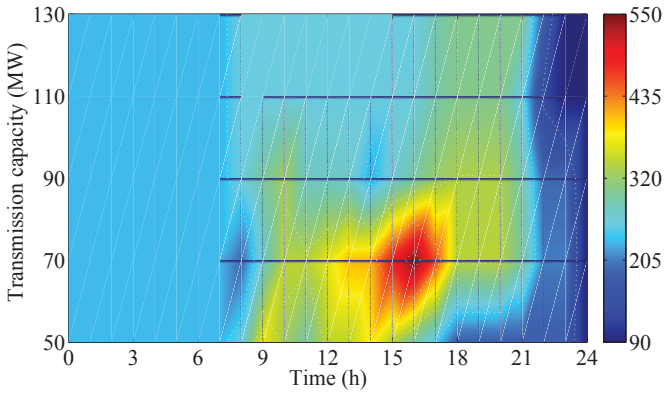

Figure 6: Thermal energy storage for transmission capacities over the time horizon.

A comparison for $\chi = 60$ MW between the results obtained in Case 1 and 2 shows that the maximum achievable profit (83,527 €) is obtained for Case 2. An increase in profit, almost 80%, is attained with the Case 2 over the Case 1. This increase in profit is due to the coordination benefits, which significantly decrease the level of uncertainty of the total power output as well as plays a vital role in enabling large amounts of wind power to be sold in the day-ahead market.

5 Conclusions

An optimization approach based on MILP is presented for the wind-CSP short-term coordination problem, in order to support the decisions of a power producer participating in the day-ahead market. A TES is effectively handled in our approach in order to improve the operational productivity of the CSP plant. Additionally, the proposed approach takes into account transmission line constraints and prevailing technical operating ones. The case studies show that: the wind-CSP plants coordination can considerably reduce generation uncertainty and may help improve the integration of more renewable energy, i.e., more CSP and wind power into a power grid. The computation time is about 10 seconds for the case studies carried out. The proposed approach is both accurate and computationally acceptable and provides an enhanced scheduling.

Acknowledgements

This work was partially supported by Fundação para a Ciência e a Tecnologia (FCT), through IDMEC under LAETA, Instituto Superior Técnico, Universidade de Lisboa, Portugal. Moreover, H.M.I. Pousinho acknowledges FCT for a post-doctoral grant (SFRH/BPD/52163/2013).

References

[1] Report: "Europe renewable energy policy handbook 2013", pp. 1–319, (2013).

[2] F. Monforti, T. Huld, K. Bodis, L. Vitali, M. D'Isidoro, R. Lacal-Arantegui, "Assessing complementarity of wind and solar resources for energy production in Italy. A Monte Carlo approach", *Renew. Energy*, **vol. 63**, pp. 576–586, (2014).

[3] H. P. Cheng, M. T. Yu, "Effect of the transmission configuration of wind farms on their capacity factors", *Energy Conv. Manag.*, **vol. 66**, pp. 326–35, (2013).

[4] D. J. Burke, M. J. O'Malley, "Factors influencing wind energy curtailment", *IEEE Trans. Sust. Energy*, **vol. 2**, pp. 185–193, (2011).

[5] H. Daneshi, A. K. Srivastava, "Security-constrained unit commitment with wind generation and compressed air energy storage", *IET Gener. Transm. Distrib.*, **vol. 6**, pp. 167–175, (2012).

[6] C.-L. Chen, "Simulated annealing-based optimal wind-thermal coordination scheduling", *IET Gener. Transm. Distrib.*, **vol. 1**, pp. 447–455, (2007).

[7] S. Kamalinia, M. Shahidehpour, "Generation expansion planning in wind-thermal power systems", *IET Gener. Transm. Distrib.*, **vol. 4**, pp. 940–51, (2010).

[8] A. A. Sanchez de la Nieta, J. Contreras, J. I. Munoz, "Optimal coordinated wind-hydro bidding strategies in day-ahead markets", *IEEE Trans. Power Syst.*, **vol. 28**, pp. 798–809, (2013).

[9] M. E. Khodayar, M. Shahidehpour, L. Wu, "Enhancing the dispatchability of variable wind generation by coordination with pumped-storage hydro units in stochastic power systems," *IEEE Trans. Power Syst.*, **vol. 28**, pp. 2808–2818, (2013).

[10] Z. Li, Q. Guo, H. Sun, Y. Wang, S. Xin, "Emission-concerned wind-EV coordination on the transmission grid side with network constraints: Concept and case study", *IEEE Trans. Smart Grid*, **vol. 4**, pp. 1692–1704, (2013).

[11] J. Usaola, "Operation of concentrating solar power plants with storage in spot electricity markets", *IET Renew. Power Gener.*, **vol. 6**, pp. 59–66, (2012).

[12] R. Dominguez, L. Baringo , A. J. Conejo, "Optimal offering strategy for a concentrating solar power plant", *Appl. Energy*, **vol. 98**, pp. 316–25, (2012).

[13] R. Sioshansi, P. Denholm, "The value of concentrating solar power and thermal energy storage", *IEEE Trans. Sust. Energy*, **vol. 1**, pp. 173–183, (2010).

[14] S. H. Madaeni, R. Sioshansi, P. Denholm, "Estimating the capacity value of concentrating solar power plants with thermal energy storage: A case study of the southwestern united states," *IEEE Trans. Power Syst.*, **vol. 28**, pp. 1205–1215, (2013).

[15] J. P. S. Catalão, H. M. I. Pousinho, V. M. F. Mendes, "An artificial neural network approach for short-term wind power forecasting in Portugal', *Eng. Intell. Syst. Electr. Eng. Commun.*, **vol. 17**, pp. 5–11, (2009).

[16] National Renewable Energy Laboratory, USA, Solar Advisor Model User Guide for Version 2.0, 2008. [Online]. Available: http://www.nrel.gov/docs.

[17] Market operator of the electricity market of the Iberian Peninsula, OMEL, 2014. [Online]. Available: http://www.omel.es.

[18] J. Ostrowski, M. F. Anjos, A. Vannelli, "Tight mixed integer linear programming formulations for the unit commitment problem", *IEEE Trans. Power Syst.*, **vol. 27**, pp. 39–46, (2012).

[19] Cplex, Gams, The solver manuals. Gams/Cplex, 2014. [Online]. Available: http://www.gams.com.